



# MRI in diagnostics of failing cerebral perfusion

PAVEL KALVACH<sup>1</sup>  
JIŘÍ KELLER<sup>2</sup>

<sup>1</sup>Department of Neurology, 3rd Medical Faculty, Charles University, Prague

<sup>2</sup>Department of Neurology, 3rd Medical Faculty, Charles University, Prague, and Department of Radiology, Hospital Na Homolce, Prague

**Correspondence:**

Prof. Pavel Kalvach, MD  
Department of Neurology,  
3rd medical faculty, FNKV  
Šrobárova 50, 100 34 Prague 10  
Czech Republic  
E-mail: kalvach@fnkv.cz

## Abstract

*Background and Purpose:* The employment of Magnetic resonance (MR) in investigations of cerebral tissue in health and disease achieved during the last 3 decades great appreciation. Its spectacular results in MR imaging and spectroscopy are especially useful in the domain of brain ischaemia.

*Materials and Methods:* We have combined practical experience with search in literature to create a review of possible examinations in the field of stroke and chronic cerebrovascular insufficiency.

*Results and Conclusions:* Our survey contains chapters on the causes of cerebral ischaemia, described in methods of MR angiography and Perfusion weighted imaging and chapters on the consequences of ischaemia: Imaging of the ischaemic cascade by classical spin echo sequences, imaging of diffusion, of contrast enhancement and distinction of the surviving parts in the hypoperfused regions. Magnetic resonance spectroscopy is reported in its proton and phosphorus examinations. Longlasting diminution of cerebral blood flow with aging is reviewed in the last chapter.

## INTRODUCTION

Magnetic resonance imaging (MRI) and Magnetic resonance spectroscopy (MRS) are two extremely valuable methods for studying the brain tissue in health and disease. In this article they are reviewed in their principles and in clinical applications for diagnostics of both acute and chronic deterioration of cerebral perfusion. In particular different modes of MR imaging are described in their employment for assessing the:

- 1 state of the big arteries on the neck and in the basal arterial circle of Willis
- 2 quality of microvascular cerebral perfusion
- 3 impact of insufficient cerebral blood flow (CBF) on tissue deterioration
- 4 appreciation of the salvageable tissue of ischaemic penumbra
- 5 investigations of chronic CBF failure producing leukoaraiosis and silent brain infarctions (SBI)

In contradistinction to historically preceding imaging methods (e.g. SPECT, CT, PET) in which the presence of different elements and compounds in the tissue was depicted, the MR resides in detecting the behaviour of the present hydrogen atoms (protons). Although the proton density is a criterion as well, those are mainly the return velocity of excited rotating protons to their resting state (T1 – relaxation) and

the homogeneity (coherence) of excited proton populations ( $T_2$  – relaxation) which are decisive for the resulting signal. Thus the electromagnetic manipulations demonstrate contrasts of different tissues in dependence on their content of free versus bound water, its intracellular or extracellular location, fixation of hydrogen by paramagnetic compounds etc. It will be shown below, that also the mobility of water molecules is detectable and concentration changes of haemoglobin vs deoxyhaemoglobin could be demonstrated.

The basic physical principles of MRI, so much important for understanding the picture and the spectroscopic curve, should be studied in textbooks. We go directly over to the methodology of the five points above. The search for the causes and the consequences of CBF failure is sometimes listed as a mnemotechnic »P quartet«: Pipes, Perfusion, Parenchyma and Penumbra (1). All these aspects are well depictable by different MRI techniques.

### A. Magnetic resonance angiography (MRA)

Arteries are visible already on routine spin-echo images. Their black appearance is produced by a so called »void of signal«. Detection of any voxel characteristics in MRI is possible only by application of two radiofrequency pulses: first excitation, then measurement of the relaxation progress. Only protons remaining in their imaging volumes would be visualized. From protons leaving the layer with the rapid arterial flow no signal is collected. The void is expressed more intensively when using long echo times. Stenotic or thrombotic lesions may be suspected in this way, and arteriovenous malformations are readily seen on such non-contrast MR scans. Also giant aneurysms (> 1,5 cm in diameter) are visible.

On the other hand short echo times combined with an absent  $180^\circ$  radiofrequency (rf) pulse, being used in gradient-echo (GRE) sequences, produce a »flow enhancement« phenomenon. This technique is useful in assessing intracranial sinus thrombosis.

Special MRA techniques base on two different principles. Both can be employed in a two- or three-dimensional acquisition technique (acquiring slices in serial or parallel manner) and viewed as both source datasets as well as 3D reconstructions.

#### a. Time of flight (TOF) MRA.

The imaging time ranges between 5 and 7 minutes, depending on the number of slices. Non-saturated spinning protons within the artery enter the surrounding static tissue, which has been magnetically manipulated (presaturation) by repeated impulses of a short repetition time (25–30 ms). The flowing blood thus appears much brighter than the stationary tissue. This »flow – related enhancement« occurs in arteries, oriented perpendicularly to the examined contiguous thin sections. For the carotid and vertebral arteries the images are acquired in the axial plane. The limited volume of such an examination is called slab. For 3-dimensional TOF MRA several slabs

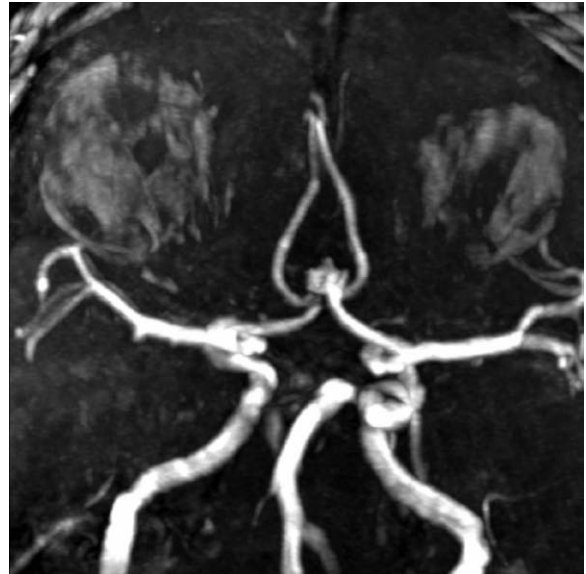


**Figure 1.** The Willis circle viewed from above. MOTSA technique of TOF MRA. An aneurysm on the anterior communicating artery.

are composed together using a MOTSA (multiple overlapping thin slab acquisition) technique (Fig. 1). Slow flow areas may not be well visualized, similarly as also the slower parts of the laminar flow could cause artifacts.

#### b. Phase contrast (PC) MRA

In this method phase shifts are imparted to moving protons by application of bipolar phase-encoding gradients. As a result high contrast angiograms are provided. Moreover a velocity encoding (VENC) can be applied to depict either arteries or veins. A faster VENC factor (60–80 cm/sec) visualizes arteries, a slower VENC (20 cm/sec) highlights the veins and sinuses (2). This method also allows to analyse collateral flow adjustments by displaying the direction of flow. The imaging time can be around 3 minutes.

#### c. Contrast enhanced (CE) MRA

Due to the intravenous application of Gadolinium chelate this MRA is less innocent to the patient, brings however a higher quality of images. It is convenient for as large fields of view as from the aortic arch up to the base of the brain. Its principle dwells in shortening the  $T_1$  relaxation in presence of Gd-DTPA (diethylenetriamino-pentaacetic acid) during its first pass through the blood vessels. It visualizes better than TOF or PC techniques the areas of slow flow behind arterial stenoses. TOF and PC MRA namely loose signal in poststenotic segments due to saturation effects and in large voxels also due to intravoxel dephasing.

Gd enhanced MRA distinguishes better thrombi as defects in the intraluminal filling. On TOF images thrombi filled up with methaemoglobin could simulate flow, as a consequence of the short  $T_1$  relaxation time of methaemoglobin.

## B/ MR Perfusion weighted imaging (PWI)

Similarly with the principle of CT perfusion measurements MRI perfusion studies detect the distribution of contrast during its first passage through axial layers of the brain. The amount of the increasing and then decaying contrast being washed out of the parenchyma needs to be modelled using the signal intensity changes in a major artery (arterial input function, AIF). Variables of cerebral perfusion present as cerebral blood flow (CBF), cerebral blood volume (CBV) and mean transit time (MTT). They are expressed best as proportion of the contralateral mirror regions of interest (ROI).

**Cerebral blood flow** can be separately measured in the gray and white matter, but their absolute values in literature differ considerably; e.g. between 37 and 94 for the gray and between 22 and 19 mL/100 g/min for the white matter respectively (3, 4).

Perfusion measurements detect the cause of the imminent ischaemic damage, as well as its stages. The ischaemic core can be distinguished from the penumbra and its particular parts – those facing recuperation and those facing a further decay. Reductions of perfusion decide whether the tissue would undergo an apoptosis or would deteriorate necrotically to malatic colliquation. In a Danish study the following CBF reductions (compared with the contralateral CBF) were found for these respective ischaemic zones: central core sentenced to later necrosis – to 26%, the penumbra part, facing later also infarction – to 42%, the penumbra benign zone, facing healing – to 62% (5). These values correspond with animal experiments, where e.g. 2 hours after an ischaemic stroke in rats values of 18 mL/100 g tissue/min and 31 mL/100 g/min were found in the ischaemic core and in the penumbra respectively (6).

**Cerebral blood volume (CBV)** is a much less reliable variable. It undergoes bimodal changes. Its decrease below 70% of the mirror healthy ROI predicts irreversible damage, but due to vasodilatory reactions to the low acidic pH the CBV fluctuates.

The most efficiently used value representing the cerebral passage of blood is »time to peak (TTP)« – an interval to the highest concentration of contrast during its passage. Prolongations of the TTP up to 1,63 of the contralateral mirror ROI should be understood as a threshold for the fatal development of the particular part of the brain tissue (5). Having in mind the physiological transit passage through the brain (3,2–3,5 sec), such a prolongation would make about 5 seconds.

**Arterial spin labeling (ALS)** is a new CBF measurement of great refinement. The spinning protons are marked by a radiofrequency impuls on the neck and consequently detected on their inflow through the brain parenchyma. Differences of the extent of 1ml/100 g/min in CBF should affect the MRI signal by a magnitude of 1%, which enables direct quantification of this measure. Moreover, ALS could be used not only for studies of a deteriorated CBF (Fig. 5, 8), but also for functional MR (7).

## C. Imaging the ischaemic cascade in the deteriorating tissue

Parenchymal suffocation following a perfusion failure presents in different degrees of its intensity. From an exclusive neuronal loss, over common death including astro- and oligodendrocytes, to a full colliquation necrosis. It has also several stages in time. The maturation of the lesion can be visualized by four different examining modes:

### a. Classical spin echo sequences.

Before signal changes develop some features of cerebral swelling may be apparent: loss of sulci (sulcal effacement) on the convexity, slight thickening of gyri and loss of distinction between the gray and white matter signal. In the initial stage the accumulation of water and its liberation from complex compounds causes first an increase of signal in T2WI and in proton density images (PDI). The increase in time versus the contralateral healthy tissue and versus cerebrospinal fluid signal is shown in Fig. 2. The yield of this spin-echo imaging is however in the last years eclipsed by measuring diffusion as an hyperacute proof of the developing infarction.

### b. Diffusion weighted imaging (DWI)

In principle the method depicts changes in Brownian molecular motion, occurring in the order of  $10^{-3}$  mm<sup>2</sup>/s. The value for water at 37°C is  $3,2 \times 10^{-3}$  mm<sup>2</sup>/s. In the cerebrospinal fluid, due to its slightly higher viscosity it makes  $2,8 \times 10^{-3}$  mm<sup>2</sup>/s (8). In the tissue diffusivity is moreover influenced by the size of the cells and of the interstitial spaces. In axonal bands and their myelin sheaths diffusion is mainly oriented longitudinally along the tracts, thus causing anisotropy of diffusion.

Diffusion-weighted images can be obtained by application of coupled gradient pulses between standard radiofrequency pulses of a classical T2-weighted imaging. The dephasing and the following rephasing of atoms affects only those ones, which had not escaped from the field during the pulses. Quickly travelling molecules would disappear and are no more detected. An

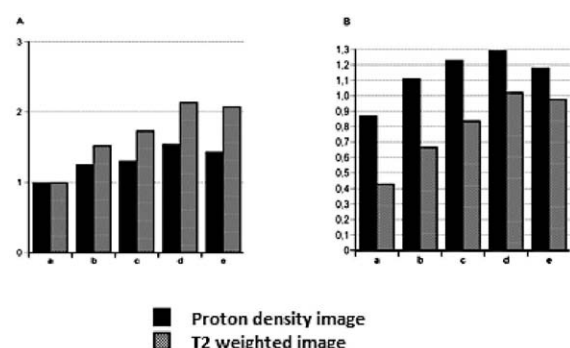


**Figure 2.** Signal development of infarcted tissue in Proton density imaging and T2 weighted imaging. A/ Brain infarction versus contralateral healthy tissue. B/ Brain infarction versus cerebrospinal fluid signal. a/ normal, b/ first 36 hours, c/ 1,5–14 days, d/ 15 days – 2 months, e/ after 2 months.

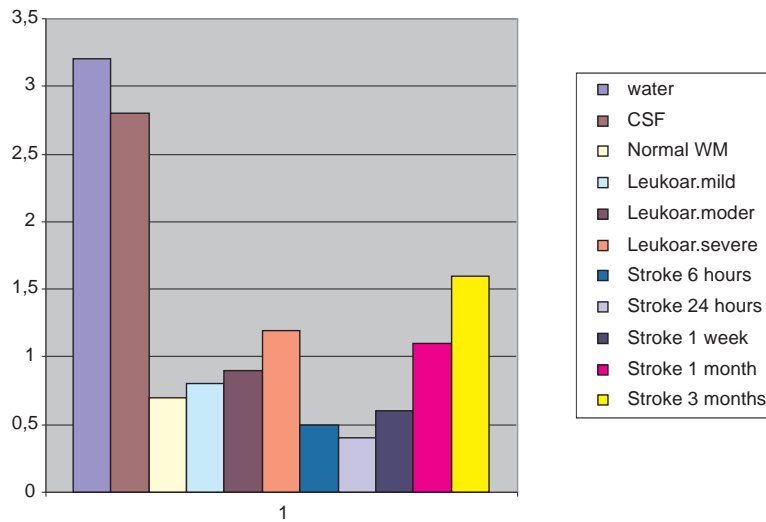


**Figure 3.** Values of diffusion in water, cerebrospinal fluid, normal white matter, mild, moderate and severe leukoaraiosis and in 5 different time intervals of ischaemic stroke. ADC values  $\times 10^{-3} \text{ mm}^2/\text{s}$ .

image weighted by diffusion is always influenced by the T2 relaxation, an inherent component of the imaging process. Presence of this variable in the final result is called a »T2 shine through«. An exact extent of diffusion can be determined only by measuring a so called Apparent Diffusion Coefficient, ADC (9). The values of ADC in a healthy brain parenchyma compared to water are 4times lower – typically  $0,76\text{--}0,77 \times 10^{-3} \text{ mm}^2/\text{s}$  (Fig.3).

DWI is the most sensitive techniques in the detection of acute stroke. The changes start first in the gray, later in the white matter. While the causes of the parenchymal damage can be determined using PWI or PET (CBF, Cerebral Metabolic Rate of Oxygen – CMRO<sub>2</sub> and Oxygen Extraction Fraction – OEF), the extent of the lesion is defined by DWI. The trigger for it is intracellular oedema with the shrinkage of the interstitial space. After the collapse of the energy dependent Na/K pump on the cytoskeleton water molecules penetrate into the intra-

cellular compartment, where their cytoplasmic mobility is reduced. Simultaneously the narrowed intercellular spaces become more tortuous. Decreased diffusion in the brain can be observed as soon as 11 minutes after the onset of a sudden CBF failure (10).

The decrease of the ADC continues in lesions without reperfusion some 3 days. Then the trend reverts, diffusion increases again – due to the development of extracellular oedema – and on days 10–14 the phenomenon achieves pseudonormalization (11), (Fig. 4).

For understanding the meaning of diffusion the metabolic thresholds of ADC changes need to be considered. ADC drops by 10% correspond with tissue acidosis and drops by 23% with a complete depletion of ATP (6). Similar correlation was also observed in time fluctuations of the extent of the DWI abnormalities after reperfusion (12).

A number of studies attempted to distinguish which values of the ADC are critical and would define a tissue with an irreversibly lost vitality. In their retrospective analysis of 48 patients with acute stroke not treated by thrombolysis Oppenheim with co-authors correlated the definitive infarction (defined by FLAIR) with zones of infarct growth from penumbra and with oligaemic zones on PWI, resulting into recovery. The ADC cutoff value for recovery was  $0,74 \times 10^{-3} \text{ mm}^2/\text{s}$ , in contrast to values of  $0,82 \times 10^{-3} \text{ mm}^2/\text{s}$  in contralateral healthy tissue. The early infarcted core had values of  $0,66 \times 10^{-3} \text{ mm}^2/\text{s}$ . These values appeared to be more reliable for the discrimination of the future infarction as the values of CBF, MTT and CBV (13). Also others have found similar thresholds; e.g. ADC of a magnitude 0,75 of the contralateral values define a tissue which would relentlessly collapse into a malacia (5).

In practical clinical reading of DW images we must be always aware of the combination of diffusivity and T2-weighted changes in the developing infarction.

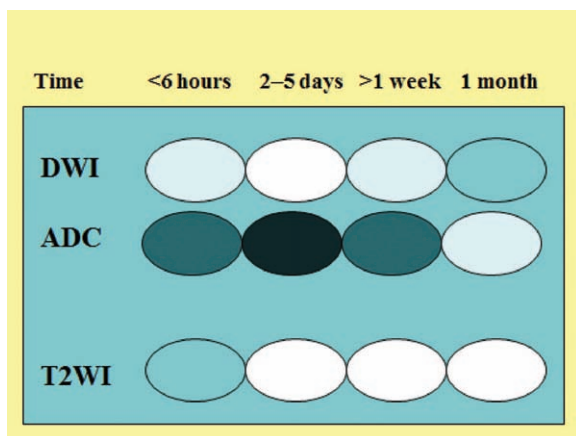


**Figure 4.** Development of 3 modalities of the MRI signal during the acute and chronic phase of stroke. DWI stays reciprocal to diffusion coefficient (ADC) and is influenced by the T2 relaxation.

Analyses of ADC in Regions of Interest (ROI) provide a good method of predicting the infarct growth area and the final infarct volume. Better than the pixel-based analyses (14). Moreover measuring the extent of districts abnormal in ADC combined with the extent of districts of prolonged mean transit time (MTT) bring more accurate information about the outcome. DWI volumes > 72 mL and NIH score > 20 were found resulting into a poor outcome, while MTT pathological volumes < 47 mL and NIH score < 8 had good outcomes (15).

Does MRI supported knowledge about the character of an ischaemic lesion at admission provide useful instructions for thrombolysis? Yes, an MRI based thrombolysis in 5 European centers within and beyond 3 hours after stroke onset, comparing CT-based decisions in a cohort of 1210 persons documented that the MRI based thrombolysis was safer and more efficacious for proper strategy (16).

### c. Contrast enhancement of ischaemic lesions

Under physiologic circumstances the capillary wall in the brain doesn't allow such compounds like Gadolinium (Gd) contrast media, or in CT investigations the Iodine contrast media to penetrate into the interstitial space. This is secured by a healthy Blood Brain Barrier (BBB). Unlike in the somatic tissues with gap junctions on the endothelial surface of the capillaries, the cerebral capillaries are equipped with tight junctions and with a firmer basal membrane. Moreover cerebral capillaries are tightly embraced by astrocytic pseudopodia and thus their interface with the parenchyma regulates selectively any transport from the vascular compartment into the interstitium. No more however after an ischaemic damage to the capillary wall. With a delay of several hours till days after the neuronal death also the BBB becomes defective. Diagnostic intravenous application of Gd-DTPA allows to distinguish those parts of the infarction, which are recanalized and enjoy perfusion from those which are not and from the healthy brain. Positivity of this phenomenon could last from usually the 2nd – 3rd day post-stroke until sometimes 50 days. During that period it can change its localization within the malacia due to different districts of restored perfusion.

The same mechanisms of BBB disruption govern also the escape of erythrocytes into the parenchyma, giving rise to its haemorrhagic transformation. The white malacia develops in this way into a red one.

In the contrast enhanced district not the Gd itself is being depicted, but its paramagnetic effects on the neighboring protons.

### d. Comparison of PWI with DWI – match or mismatch status.

In the insufficiently supplied region of the brain can be found districts of mild hypoperfusion, not yet influencing the metabolism itself (»oligaemic regions«), districts of perfusion reduced below the thresholds of membrane potentials preservation, but still with an intact intra-

cellular mitochondrial turnover (silenced function of the penumbra region) and districts with perfusion below the thresholds of neuronal vitality, defining the irreversibly devitalized core of the infarction. The penumbra zone is our field of hopes, a salvageable area providing our treatment would successfully enhance its perfusion. Therefore our knowledge of its presence and duration in particular cases is substantial.

The general guidelines for thrombolysis instruct physicians all over the world, that the time window should be rigorously maximally 4,5 hours. However, this rule is derived from clinical studies, which were unaware of any penumbra duration in individual instances. In 1999 Jean Claude Baron published his observation, that 1/3 of patients with ischaemic stroke exhibit large volumes of the penumbra even 18 hours after the stroke onset. Similarly Falcao found in his PET studies using F-FMISO in 2004 a median for the penumbra as long as 16,5 hours. Consequently it is of great advantage to know the proportion between the deadly injured ischaemic core and the struggling surroundings. The tissue within the penumbra is in fact clinically also rendered silenced in the particular moment.

Several recently published studies showed, that MRI guidance of thrombolysis refines the treatment up to 6 hours after the onset of stroke (17,18). Ribo with co-authors studied differences in safety and efficacy of rTPA treatment in a group of 135 patients who met MRI – based criteria within and after 3 hours (3–6 hours). Improvement in NIHSS, dropping by 6,3 and 6,1 points in these groups respectively and an even higher benefit in the group of late rTPA application proved that an MRI guided thrombolysis allows valuable strategic planning (19).

The combination of perfusion and diffusion studies provides nice imaging of the differently affected districts (Fig. 6). However, who wants to deliberate more precisely about the character of the regions with decreased cerebral perfusion, should also keep in mind, that the oligoemic region doesn't always need to be of primary origine. The pathophysiological concept of diaschisis (20) teaches us, that also those parts of the brain which are deprived of their standard neuronal input, suppress their metabolism and consequently also their cerebral blood flow (CBF). Clear distinction for such a mechanism could be derived for instance in case of a decreased contralateral cerebellar CBF. Due to its distance from the hemisphaeric primary lesion the diminished cerebellar blood flow can be easily deciphered as a crossed cerebellar diaschisis. Although the same mechanism is also present within the cerebral hemispheres (e.g. thalamo-cortical diaschisis, temporo-frontal diaschisis) the oligoemic regions are practically undistinguishable from a primary blood flow insufficiency. In fact the diaschitic reduction of CBF affects anatomically connected regions, which only experience suppression of their connectivity. The onset of diaschisis takes only several tens of seconds (21, 22).

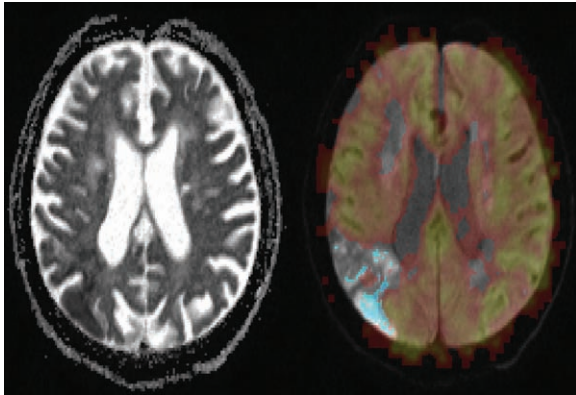


**Figure 5.** Diffusion-perfusion mismatch. On the ADC map on the left side is a chronic (high ADC) ischaemic lesion in the right frontal lobe and an acute (low ADC) lesion in the right temporo-occipital region. The right picture represents superposition of a diffusion-weighted (DWI) image with high signal in the T-P region with a cerebral blood flow (rCBF) map obtained by arterial spin labeling (ASL). The red and yellow CBF areas enjoy physiological rCBF, the gray T-P district suffers hypoperfusion. The blue colour in the DWI represents an area of  $ADC < 0.6 \times 10^{-3} / \text{mm}^2 / \text{s}$ , suggesting the core of infarction.

### D. MR Spectroscopy of cerebral ischaemic lesions

Magnetic resonance spectroscopy (MRS) did not achieve such a broad usage as imaging. Nevertheless it brings rich pieces of knowledge about chemically specific non-invasive data from the healthy or deteriorating brain tissue. It can measure concentrations of  $^{31}\text{P}$ ,  $^1\text{H}$  or  $^{13}\text{C}$  in a variety of interesting compounds. In the clinical settings, proton spectroscopy is used most often, as it has the highest signal and can be readily used in 1.5 scanners with a standard coil. The resulting curves demonstrate the amount of signal in various frequencies; frequency

shift is expressed in units called ppm (parts per million). Concentration of a given metabolite is not equal to the peak height (i.e. signal), but to the area under curve. Precise fitting of the data with a metabolite model is therefore crucial. MRS fitting is offered by scanner manufacturers as well as from third parties (Tarquin, LC model etc). In the topic of cerebral infarction the most important investigations run as spectroscopy of lactate and N-acetylaspartate (using  $^1\text{H}$ ) and as spectroscopy of the organic and inorganic phosphorus.

#### a. MRS of lactate and N-acetylaspartate.

The ubiquitous water needs to be erased from the curve by selective presaturation. In normal brain tissue the tallest peak belongs to the N-acetylaspartate (N-AA). To the left of this peak present compounds with higher ppm values, namely choline, phosphocreatine and creatine in a common peak and peaks of glutamine and glycine. To the right of the N-AA we find peaks of lipids and lactate (Fig. 6). With an insufficient oxygenation a collapse of the aerobic glycolysis is accompanied with diminution or disappearance of the phosphocreatine and creatine deposits. In the same time it brings about a switch to the agonal anaerobic glycolysis (which rises up to 700–900%) and lactate increases from its physiologically negligent levels up to 10 mmol/g within the first 10 minutes and up to 36 mmol/g in the next hours (23). Severe ischaemia breaks also mitochondrial metabolism and the peak of N-acetylaspartate disappears (Fig. 6 b).

#### b. MRS of the organic and inorganic phosphorus

The atom cores of phosphorus precede with different frequency in the compounds of phosphocreatine, adenosinotriphosphate and in the inorganic phosphorus. The peaks of these compounds profoundly change with the acute failure of oxygenation. The other peaks, namely of phosphomonoesters (mainly phosphoethanolamin) and

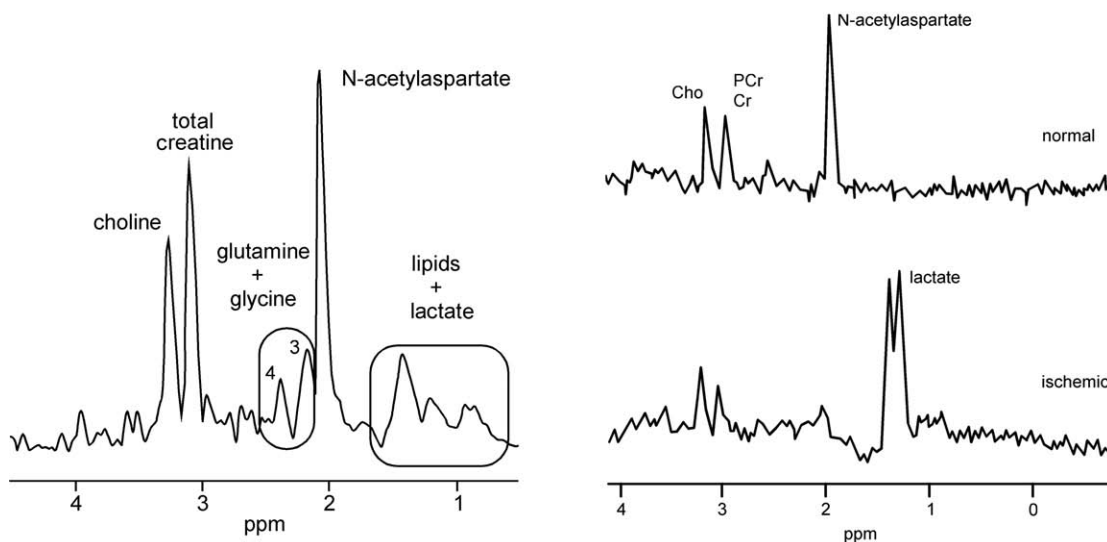


**Figure 6.** Proton MRS in healthy brain tissue (a) and comparison of normal state vs severe ischaemia in an experimental vascular occlusion model (b).

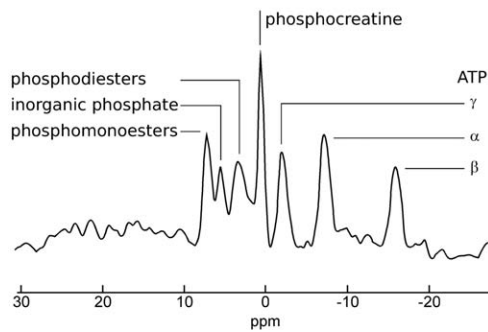


Figure 7. Physiologic spectrum of  $^{31}\text{P}$ .

phosphodiester (glycerol 3-phosphorylcholin and glycerol 3-phosphoryletanolamin) (Fig. 7) are more resistant in the acute stage, but with the developing malacia after a severe hypoxic lesion they would disappear as well. The relation of phosphocreatine to the inorganic Phosphorus is sometimes used as an index of the »mitochondrial oxidative phosphorylation function«. In the acute stage of the infarction a close correlation between pH and the levels of the inorganic phosphorus and that of phosphocreatine can be registered. However, these promising biomarkers are limited to sites equipped with a special coil for phosphorus imaging, which is not common.

### E. Chronic cerebrovascular insufficiency

With ageing cerebral tissue suffers also small ischaemic defects, which remain under the threshold of subjective attention. They used to remain also under the threshold of detection on CT. Only with the advent of MRI, especially the sequence of fluid attenuated inversion recovery (FLAIR) they became a common component of

discrete findings in aged brains. In functionally less engaged anatomical territories such small structural lesions occur inapparently and therefore are called »silent brain infarctions (SBI)«. Much more frequently they are found in the white matter, and under a general name »white matter lesions (WML)« they are often studied as a correlate to chronic (progressive) mental or motor disorders. They are miniature foci of oedema or demyelination, sometimes solitary, sometimes clustered around the frontal and/or occipital horns. Alternatively they could form periventricular lucencies. Dependent on the severity of tissue disintegration such lesions could necrotize down to a full colliquation and present as a lacune. In instances of only partial ischaemic damage these regions remain still integrated but cause a rarefaction of the white matter. Their signal increases in T2-weighted and in FLAIR images; much less is apparent their signal decrease in the T1-weighted images. The resulting picture is called leukoaraiosis (Fig. 8). In a certain aspect it means a synonymum with morbus Binswanger, or with the Olszewski's term subcortical atherosclerotic leukoencephalopathy. The extent of these changes correlates positively with cognitive disturbances and memory deficits, however the correlation coefficients are low. In the American Cardiovascular Health Study white matter lesions in 3301 persons over 65 years, without any apparent stroke, were examined by Expanded Minimal State Examination and by a Digit Symbol Substitution Test. The correlation coefficients made only 0,11 and 0,12 respectively (25).

Structural white matter lesions – periventricular hyperintensities in T2WI and deep white matter lesions – correlate in clinical aspects also with shorter survival time/risk of death, with disabilities in activities of daily living, gait disorders, with night time confusions and cerebro- and cardiovascular risk factors. In the histolo-

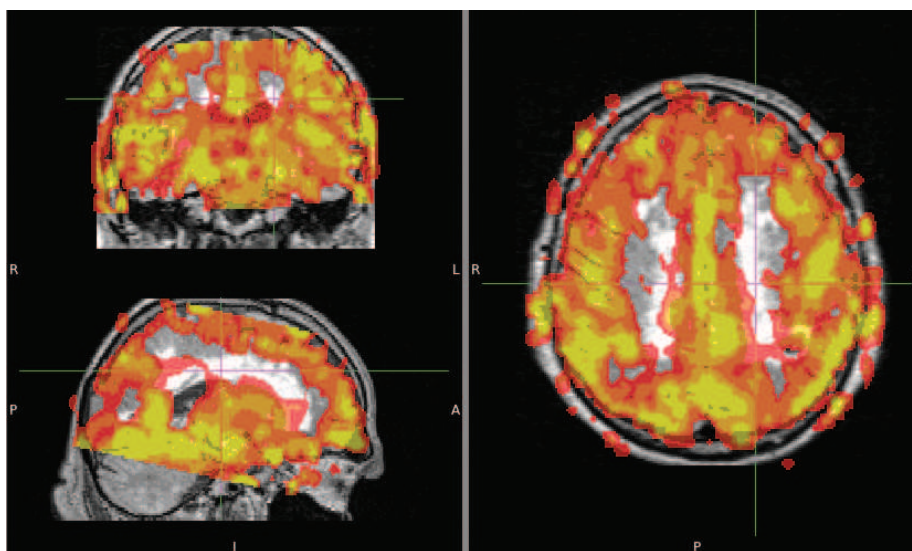
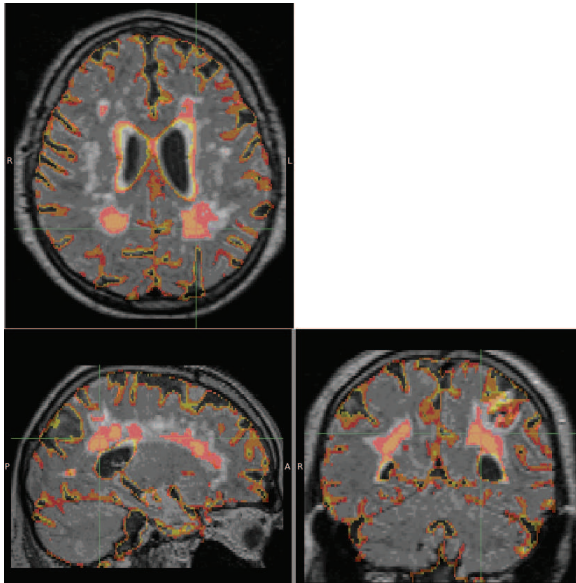


Figure 8. Association of white matter lesions on FLAIR images with districts of low cerebral blood flow (CBF). Arterial spin labeling CBF values between 35 and 75 mL/100 g/min (yellow and orange) cover major parts of cerebral hemispheres. Regions of white matter lesions have CBF below this magnitude.



**Figure 9.** Maps of Apparent Diffusion Coefficient (ADC) superimposed over the MRI FLAIR pictures in axial, sagittal and coronal views. The red and yellow colors are defined for regions of ADC between  $1,1$  and  $1,8 \times 10^{-3} \text{ mm}^2/\text{s}$ . The increased diffusion correlates with white matter hyperintensities of leukoaraiosis.

gical aspect they appear to be connected with arteriosclerosis/fibrohyaline deposits, with capillary endothelial activation and microglial activation. From the neurological point of view changes on DWI and in ADC in leukoaraiotic districts are found. We have studied relationship of WML with haemodynamics, tested by breath holding and hyperventilation. We have found a low positive correlation with the breath holding index and with the extent of vasoconstriction after hypocapnia. However a closer relationship was observed with the resistance index (26).

Our measurements of CBF using arterial spin labeling (ASL) demonstrated a clear distinction between normally perfused parts of cerebral hemispheres and the hypoperfused districts of white matter hyperintensities (Fig.8).

Transient ischaemic attacks (TIA) are often accompanied by small structural lesions detectable on diffusion-weighted images (27, 28) and contribute to the progress in leukoaraiosis. Other TIAs are accompanied with deficits only in perfusion-weighted studies (29).

We have examined persons with leukoaraiosis using FLAIR images and ADC maps aiming at realizing whether the white matter hyperintensities would be accompanied with increased diffusion. This association appeared to be evident (Fig.9).

MRI studies also allowed to investigate cerebral perfusion and cerebrovascular reactivity not only in the whole hemisphere, but also selectively in the gray and white matter. In districts of white matter hyperintensities perfusion as well as vascular reactivity were found decreased compared to the normal appearing white matter

(30). Moreover in another study the authors disclosed, that during cortical activation the enhanced CBF to the cortex in the experiment of functional MRI is associated with a decreased and insufficient CBF to the white matter. This finding is most apparent in vascular borderzones and in white matter periventricular lesions, suggesting a deleterious steal phenomenon during activations under conditions of a limited cerebral blood supply (31).

*Acknowledgement:* This paper was produced using a Research project MSM PRVOUK P34.

## REFERENCES

1. ROWLEY H A 2001 The four Ps of acute stroke imaging: Parenchyma, Pipes, Perfusion, and Penumbra. *AJNR* 22: 599–601
2. HESSELINK J R. MR angiography: CNS applications. <http://spinwarp.ucsd.edu/neuroweb/Text/MR-ANGIO.htm>
3. KOSHIMOTO Y, YAMADA H, KIMURA H *et al.* 1999 Quantitative analysis of cerebrovascular hemodynamics with T2-weighted dynamic MR imaging. *J Magn Reson Imaging* 9 (3): 462–467
4. HELENIUS J, PERKIO J, SOINNE L *et al.* 2003 Cerebral hemodynamics in a healthy population measured by dynamic susceptibility contrast MR imaging. *Acta Radiol* 44(5): 538–546
5. ROHL L, OSTERGAARD L, SIMONSEN C Z *et al.* 2001 Viability thresholds of ischemic penumbra of hyperacute stroke defined by perfusion-weighted MRI and apparent diffusion coefficient. *Stroke* 32: 1140–1148
6. HOEHN-BERLAGE M, NORRIS D G, KOHNO K, MIES G, LEIBFRIITZ D, HOSSMAN K-A 1995 Evolution of regional changes of apparent diffusion coefficient during focal ischemia of rat brain – the relationship of quantitative NMR imaging to reduction in cerebral blood flow and metabolic disturbances. *J Cereb Blood Flow Metab* 15: 1002–1011
7. WANG J J, AGUIRRE G K, KIMBERG D Y *et al.* 2003 Arterial spin labeling perfusion AM with very low task frequency. *Magn Res Med* 45(9): 796–802
8. HELENIUS J, SOINNE L, SALONEN O, KASTE M, TATLISUMAK T. 2002 Leukoaraiosis, ischemic stroke and normal white matter on diffusion-weighted MRI. *Stroke* 33: 45–50
9. MORITANI T, EKHOLM S, WESTESSON P L Diffusion-weighted MR imaging of the brain. Springer 2005, Berlin-Heidelberg-New York, p 230
10. Hjort N *et al.* 2005 Ischemic injury detected by diffusion imaging 11 minutes after stroke. *Ann Neurol* 58(3): 462–465
11. FIEBACH J B, JANSEN O, SCHELLINGER P D, HEILAND S, HACKE W, SARTOR K *et al.* 2002 Serial analysis of the apparent diffusion coefficient time course in human stroke. *Neuroradiology* 44: 294–298
12. OLAH L, WECKER S, HOEHN M 2001 Relation of apparent diffusion coefficient changes and metabolic disturbance after 1 hour of focal cerebral ischemia and at different reperfusion phases in rats. *J Cereb Blood Flow Metab* 4: 430–439
13. OPPENHEIM C, GRANDIN C, SAMSON Y, SMITH A, DUPREZ T, MARSAULT C *et al.* 2001 Is there an apparent diffusion coefficient in predicting tissue viability in hyperacute stroke? *Stroke* 32: 2486–2491
14. NA D G, THIJS V N, ALBERS G W, MOSELEY M E, MARKS M P 2004 Diffusion-weighted MR imaging in acute ischemia: Value of apparent diffusion coefficient and signal intensity thresholds in predicting tissue at risk and final infarct size. *AJNR* 25: 1331–1336
15. YOO A J, BARAK E R, COPEN W A, KAMALIAN S, GHARAI L R, PERVEZ M A, SCHWAMM L H *et al.* 2010 Combining acute diffusion weighted imaging and mean transmit time lesion volumes with National Institutes of Health stroke scale score improves the prediction of acute stroke outcome. *Stroke* 41: 1728–1735
16. SCHELLINGER P D, THOMALLA G, FIEHLER J, KÖHRMANN M, MOLINA C A, NEUMANN-HAEFELIN T, RIBO M, SINGER O C, ZARO-WEBER O, SOBESKY J 2007 MRI-based and CT-based thrombolytic therapy in acute stroke within and beyond established time windows. An analysis of 1210 patients. *Stroke* 38: 2640–2645



17. ALBERS G W, THIJIS W N, WECHSLER L *et al.* 2006 Magnetic resonance imaging profiles predict clinical response to early reperfusion: the diffusion and perfusion imaging evaluation for understanding stroke evolution (DEFUSE) study. *Ann Neurol* 60: 508–517
18. DAVIS S M, DONNAN G A, PARSONS M W *et al.* 2008 Effects of alteplase beyond 3 hours after stroke in the Echoplanar Imaging Thrombolytic Evaluation Trial (EPITHET): a placebo-controlled randomised trial. *Lancet Neurol* 7: 299–309
19. RIBO M, MOLINA C A, ROVIRA A, QUINTANA M, DELGADO P, MONTANER J, GRIVÉ E, ARENILLAS J F, ÁLVAREZ-SABÍN J 2005 Safety and efficacy of intravenous tissue plasminogen activator stroke treatment in the 3- to 6-hour window using multimodal transcranial Doppler/MRI selection protocol. *Stroke* 36: 602–606
20. REIVICH M 1992 Crossed cerebellar diaschisis. *Am J Neuroradiol* 13: 62–66
21. ECKARD D A, PURDY P D, BONTE F 1992 Crossed cerebellar diaschisis and loss of consciousness during temporary balloon occlusion of the internal carotid artery. *Am J Neuroradiol* 13: 55–58
22. BRUNBERG J A, FREY K A, HORTON J A, KUHL D E 1992 Crossed cerebellar diaschisis: Occurrence and resolution demonstrated with PET during carotid temporary balloon occlusion. *Am J Neuroradiol* 13: 58–61
23. PETROFF O A C, PRICHARD J W, OGINO T, SHULMAN R G 1988 Proton magnetic resonance spectroscopic studies of agonal carbohydrate metabolism in rabbit brain. *Neurology* 38: 1569–1574
24. GRAHAM G D, BLAMIRE A M, HOWSEMAN A M *et al.* 1992 Proton magnetic resonance spectroscopy of cerebral lactate and other metabolites in stroke patients. *Stroke* 23: 333–340
25. LONGSTRETH W T, MANOLIO T A, ARNOLD A *et al.* 1996 Clinical correlates of white matter findings on cranial magnetic resonance imaging of 3301 elderly people. The Cardiovascular Health study. *Stroke* 27: 1274–1282
26. PEISKER T, BARTOŠ A, ŠKODA O, IBRAHIM I, KALVACH P 2010 Impact of aging on cerebral vasoregulation and parenchymal integrity. *J Neurol Sci.* 299: 112–115
27. WINBECK K, BRUCKMAIER K, ETGEN T, GRÄFIN VON EINSIEDEL H, RÖTTINGER M, SANDER D 2004 Transient ischaemic attack and stroke can be differentiated by analyzing early diffusion-weighted imaging signal intensity changes. *Stroke* 35: 1095–1099
28. REDGRAVE J N E, COUTTS S B, SCHULZ U G, BRILEY D, ROTHWELL P M 2007 Systematic review of associations between the presence of acute ischemic lesions on diffusion-weighted imaging and clinical predictors of early stroke risk after transient ischemic attack. *Stroke* 38: 1482–1488
29. RESTREPO L, JACOBS M A, BARKER P B, WITYK R J 2004 Assessment of transient ischemic attack with diffusion- and perfusion-weighted imaging. *AJNR* 25: 1645–1652
30. MARSTRAND J R, GARDE E, ROSTRUP E, ROSENBAUM S, MORTENSEN E L, LARSSON H B W 2002 Cerebral perfusion and cerebrovascular reactivity are reduced in white matter hyperintensities. *Stroke* 33: 972–976
31. MANDELL D M, HAN J S, POUBLANC J, CRAWLEY A P, KASSNERA, FISHER J A, MIKULIS D J 2008 Selective reduction of blood flow to white matter during hypercapnia corresponds with leukoaraiosis. *Stroke* 39: 1993–1998